First Experience Using ^{18}F-Flubrobenguane PET Imaging in Patients with Suspected Pheochromocytoma or Paraganglioma

Lukas Kessler[1], Anna M. Schlitter[2], Markus Krönke[3], Alexander von Werder[4], Robert Tauber[5], Tobias Maurer[5], Simon Robinson[6], Cesare Orlandi[6], Michael Herz[3], Behrooz H. Yousefi[3,7], Stephan G. Nekolla[3], Markus Schwaiger[3], Matthias Eiber*[3], and Christoph Rischpler*[1,3]

[1]Department of Nuclear Medicine, University Hospital Essen, University of Duisburg–Essen, Essen, Germany; [2]Institute of Pathology, Technical University Munich, Munich, Germany; [3]Department of Nuclear Medicine, Klinikum rechts der Isar, Technical University of Munich, Munich, Germany; [4]Department of Gastroenterology, Klinikum rechts der Isar, Technical University of Munich, Munich, Germany; [5]Department of Urology, Klinikum rechts der Isar, Technical University of Munich, Munich, Germany; [6]Discovery Research, Lantheus Medical Imaging, North Billerica, Massachusetts; and [7]Department of Nuclear Medicine, Philipps University of Marburg, Marburg, Germany

Pheochromocytomas and paragangliomas are a rare tumor entity originating from adrenomedullary chromaffin cells in the adrenal medulla or in sympathetic, paravertebral ganglia outside the medulla. Small lesions are especially difficult to detect by conventional CT or MRI and even by SPECT with the currently available radiotracers (e.g., metaiodobenzylguanidine [MIBG]). The novel PET radiotracer ^{18}F-flubrobenguane could change the diagnostic paradigm in suspected pheochromocytomas and paragangliomas because of its homology with MIBG and the general advantages of PET imaging. The aim of this retrospective analysis was to evaluate ^{18}F-flubrobenguane in pheochromocytomas and paragangliomas and to investigate the biodistribution in patients. **Methods:** Twenty-three patients with suspected pheochromocytoma or paraganglioma underwent PET/CT or PET/MRI at 63 ± 24 min after injection of 256 ± 33 MBq of ^{18}F-flubrobenguane. The SUV_{mean} and SUV_{max} of organs were measured with spheric volumes of interest. Threshold-segmented volumes of interest were used to measure the SUV_{mean} or SUV_{max} of the tumor lesions. One reader evaluated all cross-sectional imaging datasets (CT or MRI) separately, as well as the PET hybrid datasets, and reported the lesion number and size. The diagnostic certainty for a positive lesion was scored on a 3-point scale. **Results:** ^{18}F-flubrobenguane showed a reproducible, stable biodistribution, with the highest SUV_{max} and SUV_{mean} being in the thyroid gland (30.3 ± 2.2 and 22.5 ± 1.6, respectively), pancreas (12.2 ± 0.8 and 9.5 ± 0.7, respectively), and tumor lesions (16.8 ± 1.7 and 10.1 ± 1.1, respectively) and the lowest SUV_{max} and SUV_{mean} being in muscle (1.1 ± 0.06 and 0.7 ± 0.04, respectively) and the lung (2.5 ± 0.17 and 1.85 ± 0.13, respectively). In a subgroup analysis, a significantly higher average SUV_{mean} was seen for both pheochromocytoma and paraganglioma than for healthy adrenal glands (11.9 ± 2.0 vs. 9.9 ± 1.5 vs. 3.7 ± 0.2, respectively). In total, 47 lesions were detected. The reader reported more and smaller lesions with higher certainty in PET hybrid imaging than in conventional imaging; however, statistical significance was not reached. Of the 23 (23/47, 49%) lesions smaller than 1 cm, 61% (14/23) were found on hybrid imaging only. **Conclusion:** Our preliminary data suggest ^{18}F-flubrobenguane PET to be a new, effective staging tool for patients with suspected pheochromocytoma or paraganglioma. Major advantages are the fast acquisition and high spatial resolution of PET imaging and the intense uptake in tumor lesions, facilitating detection. Further studies are warranted to define the role of ^{18}F-flubrobenguane PET, particularly in comparison to standard diagnostic procedures such as MRI or ^{123}I-MIBG SPECT/CT.

Key Words: PET/CT; PET/MRI; F-18 flubrobenguane; PET; paraganglioma; pheochromocytoma

J Nucl Med 2021; 62:479–485
DOI: 10.2967/jnumed.120.248021

Pheochromocytomas are rare, catecholamine-producing tumors originating from chromaffin cells in the adrenal medulla or in sympathetic, paravertebral ganglia outside the medulla (the latter are usually referred to as paragangliomas) (*1,2*). Sympathetic paragangliomas may be located in the pelvis, the abdomen, or the thorax. About 80%–85% of pheochromocytomas arise from the adrenal medulla, whereas 15%–20% originate from extraadrenal chromaffin tissue (*1*). Pheochromocytomas and paragangliomas may occur in the context of genetic disorders (*3–5*). Furthermore, pheochromocytomas may be bilateral in more than 10% of cases or may even be multifocal (particularly in familial pheochromocytoma syndromes) (*1,6*). Malignancy is relatively rare in adrenal pheochromocytomas (≤5%) but is quite common in paragangliomas (≤33%) (*1,7*). There is no genetic or histologic marker that definitely indicates malignancy in these tumors; for this reason, malignancy is defined in the World Health Organization classification as being the occurrence of metastasis (*8*). Surgery is generally recommended as the primary treatment, with curative intent (*2*). These facts illustrate the immense importance of noninvasive assessment of the disease before surgery.

CT is recommended as the primary imaging modality because of a high sensitivity of about 90%, whereas MRI is recommended in special situations only (e.g., paragangliomas of the head and neck, contrast medium allergy, or young patients) (*2,9,10*). Both CT and MRI have low specificity. In contrast, iodine-labeled (^{123}I- or ^{131}I) metaiodobenzylguanidine (MIBG) scintigraphy and SPECT imaging demonstrate a high specificity ranging from 70% to 100% at an acceptable sensitivity (56%–88%) for both pheochromocytomas

Received Apr. 27, 2020; revision accepted Jul. 20, 2020.
For correspondence or reprints contact: Christoph Rischpler, Klinikum rechts der Isar, Nuklearmedizinische Klinik und Poliklinik, Ismaninger Strasse 22, 81675 München, Germany.
E-mail: c.rischpler@tum.de
*Contributed equally to this work.
Published online Aug. 28, 2020.

and paragangliomas (*2*). However, PET is usually preferred over SPECT because of the higher sensitivity and higher spatial resolution of the former, often resulting in higher diagnostic accuracy (*11*). Also, PET allows for truly quantitative imaging, facilitating response assessment (*11*), and has shorter acquisition times.

The available PET tracers for the assessment of pheochromocytoma or paraganglioma are ^{18}F-FDG, somatostatin receptor targeting tracers such as ^{68}Ga-DOTATATE, and rarely used PET tracers such as ^{11}C-hydroxyephedrine, ^{18}F-fluorodopa, ^{18}F-fluorodopamine, or ^{124}I-MIBG. However, these radiotracers have disadvantages such as a long half-life and high cost (^{124}I), the need for an onsite cyclotron (^{11}C), a complex radiosynthesis (^{18}F-fluorodopa and ^{18}F-fluorodopamine), or a low specificity for pheochromocytoma and paraganglioma (somatostatin receptor targeting tracers) (*12–14*). N-[3-bromo-4-(3-^{18}F-fluoro-propoxy)-benzyl]-guanidine (^{18}F-flubrobenguane, formerly known as LMI1195) is a novel, ^{18}F-labeled radiotracer that has a high homology with MIBG and can visualize norepinephrine transporters with a high affinity and specificity (*15*). This radiotracer has been evaluated successfully in a MENX tumor model, a rat model with bilateral pheochromocytomas (*16*). In humans, this radiotracer has been evaluated in healthy volunteers for biodistribution and radiation dosimetry studies and in a recent case report of a 74-y-old man with heart failure who underwent ^{18}F-flubrobenguane and ^{11}C-hydroxyephedrine PET (*17,18*). The aim of this retrospective analysis was to evaluate ^{18}F-flubrobenguane in patients with suspected pheochromocytoma or paraganglioma.

MATERIALS AND METHODS

Radiotracer Synthesis

^{18}F-flubrobenguane was synthesized as previously described (*15*).

Briefly, the synthesis was performed using a brosylate precursor and a 1-step no-carrier-added ^{18}F displacement reaction with high-performance liquid chromatography purification. Radiochemical purity was at least 95% in all performed syntheses, and specificity was more than 130 GBq/μmol. The radiotracer was formulated in an 8% ethanol/saline solution.

All patients gave written informed consent for the procedure as a legal requirement for ^{18}F-flubrobenguane PET/CT or PET/MRI on a compassionate-use basis. All reported investigations were conducted

TABLE 1
Patient Characteristics and Scan Details

Patient no.	Age (y)	Activity (MBq)	Time after injection (min)	Scanner	Indication for scan	Imaging result	Lesions (*n*)	
							Hybrid	CT/MRI
1	57	291	43	PET/CT	Suspicion of PHEO*	Primary PHEO†	1	1
2	45	218	46	PET/CT	Suspicion of PHEO*	Primary PHEO†	1	1
3	71	253	81	PET/CT	Clinical suspicion	Normal	0	0
4	62	183	45	PET/CT	Clinical suspicion	Normal	0	0
5	57	251	56	PET/CT	Suspicion of PHEO*	Primary PHEO†	1	1
6	38	256	58	PET/CT	PGL in history	Recurrent PGL	4	1
7	63	275	54	PET/CT	Suspicion of PHEO*	Adrenal adenoma†	1	1
8	55	290	54	PET/CT	Suspicion of PHEO*	Primary PHEO†	1	1
9	48	270	59	PET/CT	Suspicion of PHEO*	Primary PHEO†	1	1
10	63	271	52	PET/CT	PHEO in history	Recurrent PHEO	9	2
11	67	227	57	PET/CT	PHEO and PGL in history	Recurrent PHEO	1	1
12	68	262	81	PET/CT	Suspicion of PHEO*	Primary PHEO†	1	1
13	50	224	45	PET/MRI	Suspicion of PHEO*	Adrenal adenoma†	0	1
14	68	297	72	PET/CT	Suspicion of PHEO*	Primary PHEO†	1	1
15	48	302	73	PET/CT	Catecholamines in urine	Normal	2	0
16	55	213	87	PET/CT	Suspicion of PGL*	Primary PGL†	1	1
17	77	237	143	PET/CT	Suspicion of PHEO*	Primary PHEO	1	1
18	41	245	45	PET/CT	PGL in history	Recurrent PGL	3	1
19	62	254	97	PET/CT	PGL in history	Recurrent PGL†	7	6
20	56	224	76	PET/CT	Suspicion of PHEO*	Primary PHEO†	1	1
21	51	228	55	PET/MRI	Suspicion of PHEO*	Primary PHEO	1	1
22	77	233	59	PET/CT	Suspicion of PHEO*	Primary PHEO	1	1
23	56	247	57	PET/CT	Suspicion of PHEO*	Primary PHEO†	1	1

*Suspicion of pheochromocytoma or paraganglioma due to other morphologic imaging modalities.
†Patients with histopathologic result after surgery.
PHEO = pheochromocytoma; PGL = paraganglioma.
Patients 6, 11, and 19 underwent repetitive scans.

in accordance with the Helsinki Declaration and with national regulations. The retrospective analysis was approved by the local Ethics Committee (permit 142/20 S-KH). The administration of ^{18}F-flubrobenguane complied with the German Medicinal Products Act, AMG §13 2b, and the responsible regulatory body (Government of Upper Bavaria).

Patient Population and Imaging Protocol

Twenty-three patients with clinically suspected or a history of pheochromocytoma or paraganglioma underwent whole-body (head to mid thigh) PET/CT (Biograph mCT) or PET/MRI (Biograph mMR) between August 2016 and November 2018 (Table 1). Fifteen patients underwent at least one other imaging modality before ^{18}F-flubrobenguane PET (CT, 8; MRI, 9), including 4 patients whose medical history showed that they had undergone ^{123}I-MIBG SPECT/CT. In total, 26 PET scans (24 PET/CT, 2 PET/MRI [3 patients were scanned twice]) were performed after injection of a mean activity of 256 ± 33 (range, 183–307 MBq). The PET acquisition was started after 63 ± 24 min (range, 43–143 min). In PET/CT, a diagnostic CT scan in the portal venous phase was performed (Imeron 300 [iomeprol 300 mg iodine/mL, Bracco Imaging Deutschland, Konstanz, Germany] at 1.5 mL/kg of body weight). In PET/MRI, the following sequences were acquired: T1-weighted volumetric interpolated breath-hold examination (VIBE) Dixon (for attenuation correction purposes), axial and coronal T2-weighted half-Fourier-acquired single-shot turbo spin echo (skull to mid thigh), axial diffusion-weighted imaging, axial T1-weighted VIBE with contrast dynamics, and axial T1-weighted in-phase/opposed-phase, axial T1-weighted VIBE fat saturated (all upper abdomen). For contrast-enhanced MRI, a 0.2-mL dose of gadoterate meglumine (Dotarem [Guerbet], 0.5 mmol/mL) per kilogram of body weight was injected.

Quantitative and Qualitative Image Analysis

The biodistribution of ^{18}F-flubrobenguane was quantified by SUV_{mean} and SUV_{max} corrected for body weight (*19*). Spheric volumes of interest 1 cm in diameter (salivary glands, thyroid, myocardium, stomach, and pancreas) and 2 cm in diameter (bladder, liver, spleen, kidney, muscle, aortic lumen, and lungs) were placed inside the organs' parenchyma. SUV_{mean} and SUV_{max} for tumor lesions were measured by circular, 3-dimensional regions of interest at a 40% isocontour around the lesions using Syngo.via software (Siemens Healthcare).

Imaging data of the hybrid PET/CT or combined PET/MRI were read separately against the respective cross-section imaging dataset only by a dual board-certified radiologist and nuclear medicine physician. Lesion size and number were reported, and the diagnostic certainty for positive lesions was rated using the categories "possible," "probable," or "consistent with."

Additionally, in the 4 subjects who underwent both ^{123}I-MIBG SPECT/CT and ^{18}F-flubrobenguane PET/CT, imaging datasets were compared visually for divergent findings.

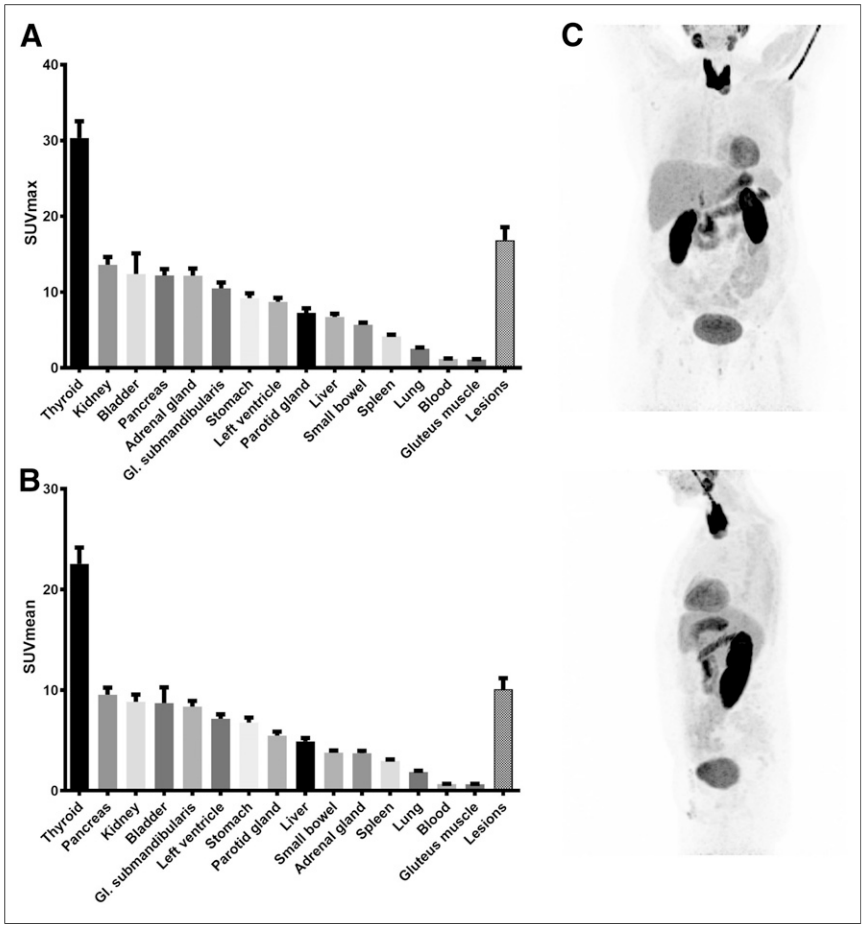

FIGURE 1. (A and B) SUV_{max} (A) and SUV_{mean} (B) of ^{18}F-flubrobenguane in organs. Highest uptake is in thyroid, pancreas, and pheochromocytoma and paraganglioma lesions. Lowest uptake is in muscle, lung, and blood pool (aortic lumen). (C) Maximum-intensity projection of negative PET scan. Gl. = glandula.

Histopathology

Thirteen patients (13/23, 57%) underwent surgery and subsequent histopathologic analysis of the tumor lesions. Eleven of those had a positive finding (11/13, 85%): 2 patients had proven paraganglioma (2/11, 18%) and 9 patients had pheochromocytoma (9/11, 82%). In 2 patients (2/13, 15%), an adrenal adenoma was diagnosed.

Statistics

Data are reported as mean ± SEM, and all statistical analysis was performed with Prism, version 8.4.2 (GraphPad Software). To compare groups, the Student t test was applied, or ANOVA was applied if more than 2 groups were compared and data were normally distributed. The Mann–Whitney test was performed for nonparametric data. Differences were considered statistically significant at P values of less than 0.05.

RESULTS

Quantitative Analysis of Biodistribution and Tumor Lesions

^{18}F-flubrobenguane showed stable and reproducible biodistribution in healthy organs. The highest SUV_{mean} was in the thyroid glands (22.5 ± 1.6), pancreas (9.5 ± 0.7), and kidneys (8.8 ± 0.7), the last of these being due to the excretion pathway of the radiotracer. Accordingly, high uptake in the urinary bladder was observed (8.7 ± 1.5). SUV_{mean} was lowest in the lungs (1.85 ± 0.13), muscles (0.7 ± 0.04), and blood pool (0.65 ± 0.03).

Lesions suspected of being pheochromocytoma or paraganglioma had very intense uptake (SUV_{mean}, 10.1 ± 1.1) that was significantly higher than uptake in liver parenchyma and healthy adrenal glands (4.9 ± 0.3 and 3.7 ± 0.24, respectively; $P < 0.0001$). SUV_{max} was 16.8 ± 1.7 versus 6.7 ± 0.4 versus 12.2 ± 0.95, respectively; $P < 0.01$) (Figs. 1 and 2A). Uptake in pheochromocytoma and paraganglioma was relatively similar (SUV_{mean}, 11.9 ± 2.0 vs. 9.9 ± 1.5, respectively [$P = 0.44$]; SUV_{max}, 19.0 ± 3.0 vs. 16.8 ± 2.1, respectively [$P = 0.55$]). When pheochromocytoma and paraganglioma were evaluated separately, tracer uptake was significantly higher than in healthy adrenal glands (SUV_{mean}, 11.9 ± 2.0 vs. 9.9 ± 1.5 vs. 3.7 ± 0.2, respectively [$P < 0.01$]; SUV_{max}, 19.0 ± 3.0 vs. 16.8 ± 2.1 vs. 12.2 ± 0.95 [$P < 0.05$]) (Fig. 2.).

Lesion Detection and Certainty

In total, 47 lesions were detected on hybrid PET/CT or PET/MRI. No statistically significant difference in number of lesions or lesion size was present. Still, a clearly higher number of lesions (1.8 ± 0.4 vs. 1.1 ± 0.2, $P = 0.24$) was reported for hybrid imaging than for CT or MRI (Fig. 3A). Especially, a smaller mean lesion size was reported for ^{18}F-flubrobenguane PET/CT or PET/MRI (1.7 ± 0.2 cm vs. 2.2 ± 0.3 cm, $P = 0.10$) (Fig. 3B). In addition, diagnostic certainty about positive lesions was superior for ^{18}F-flubrobenguane hybrid imaging, with 62.5% of lesions rated as "consistent with," 25.0% rated as "probable," and 12.5% rated as "possible," compared with 35.5%, 38.7%, and 25.8%, respectively, for CT or MRI alone (Fig. 3C).

Interestingly, of the 47 lesions detected in total, 31 (66%) were found both on cross-sectional imaging alone and on PET hybrid imaging, whereas 16 (34%) were found on hybrid imaging only. No lesions were seen only on cross-sectional imaging. Of note, 61% (14/23) of the 23 (23/47, 49%) lesions smaller than 1 cm were found on hybrid imaging only, whereas 92% (22/24) of the lesions larger than 1 cm were also detected on cross-sectional imaging (Fig. 3D).

Case Examples

Figure 4 depicts the ^{18}F-flubrobenguane PET/CT images of 2 patients. First, a 50-y-old man was referred because of an unclear lesion on conventional imaging in the left adrenal gland and a history of hypertension. ^{18}F-flubrobenguane PET/CT showed only mild tracer uptake, and surgical resection diagnosed an aldosterone-producing adenoma (Fig. 4A). In the other patient, a 57-y-old man with an elevated concentration of metanephrine in the plasma, a contrast-enhancing, centrally hypodense lesion with intense ^{18}F-flubrobenguane uptake was detected in the right adrenal gland and suspected of representing pheochromocytoma. Subsequent surgical resection and histopathology verified the imaging results. Correspondence was seen between the necrotic area within the tumor, which showed no uptake, and intense tracer uptake in the vital surrounding area (Fig. 4B). In our cohort, only 2 individuals were diagnosed with an adrenal adenoma after surgical resection; the adenomas and the healthy adrenal glands of these patients had a similar SUV_{mean} (Supplemental Fig. 1; supplemental materials are available at http://jnm.snmjournals.org).

In a third patient, who was 38 y old and had recurrent pheochromocytoma after multiple resections, ^{123}I-MIBG SPECT/CT was performed for suspected recurrence (Supplemental Fig. 2). The scan revealed suspected paravertebral lesions close to the left kidney. In a follow-up scan with ^{18}F-flubrobenguane PET/CT 6 mo later, 2 small lesions with intense ^{18}F-flubrobenguane uptake, which were not detectable on ^{123}I-MIBG SPECT/CT, could be identified in the pelvis. In another follow-up ^{18}F-flubrobenguane PET/CT scan 14 mo after the SPECT/CT, lesions were still detectable and overall stable disease was reported. Since a stable condition was previously reported over several years by means of annual ^{123}I MIBG SPECT/CT examinations, progressive disease appeared very unlikely and the reason for the additional lesions most likely lay in the superiority of ^{18}F-flubrobenguane PET over ^{123}I SPECT. However, this single case does not allow general conclusions on a comparison of the 2 tracers and imaging modalities.

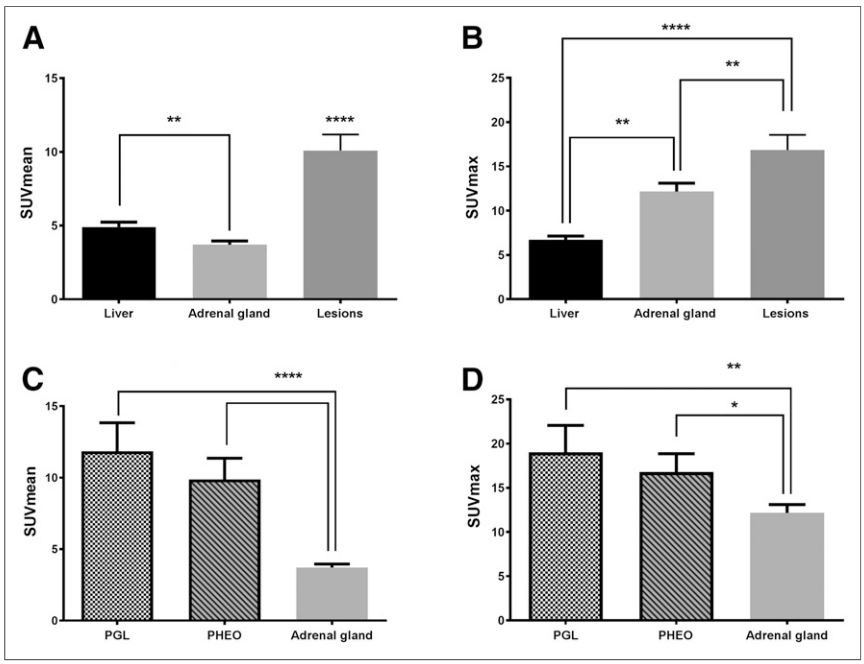

FIGURE 2. SUV_{max} and SUV_{mean} of pheochromocytoma and paraganglioma lesions, liver, and adrenal glands. (A) SUV_{mean} was significantly higher in all lesions than in liver parenchyma and adrenal glands and was significantly higher in liver parenchyma than in normal adrenal glands. (B) SUV_{max} was significantly higher in lesions and healthy adrenal glands than in liver parenchyma. (C and D) SUV_{mean} (C) and SUV_{max} (D) were significantly higher in paraganglioma and pheochromocytoma than in healthy adrenal glands and liver. *$P < 0.05$. **$P < 0.01$. ****$P < 0.0001$. PGL = paraganglioma; PHEO = pheochromocytoma.

DISCUSSION

In the present retrospective study, a novel ^{18}F-labeled PET radiotracer, ^{18}F-flubrobenguane, targeting the norepinephrine transporter was evaluated in 23 patients with clinical suspicion of, or a history of, pheochromocytoma or paraganglioma. The results demonstrated a favorable biodistribution, with pheochromocytomas and paragangliomas having intense uptake clearly above the level

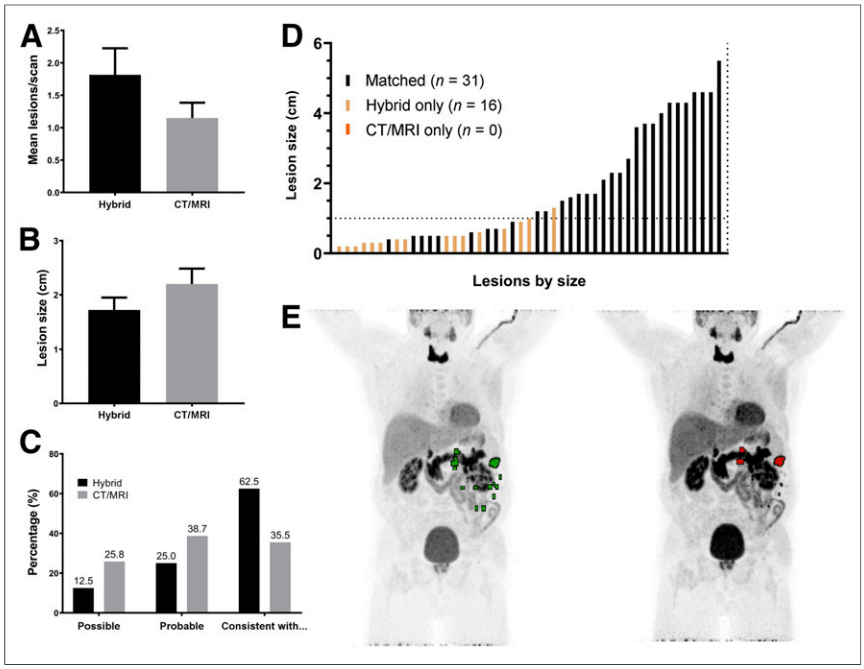

FIGURE 3. Separate and combined reading of ^{18}F-flubrobenguane PET hybrid imaging and CT or MRI. (A and B) There was no significant difference in number of lesions per scan (A) or lesion size (B) in either reading. (C) Reader certainty was higher for hybrid imaging. In total, 47 lesions were detected. (D) Most lesions were found on CT or MRI and on hybrid imaging (matched; $n = 31$). No lesion was detected on CT or MRI alone ($n = 0$), but several lesions were detected on hybrid imaging alone ($n = 16$). An increased number of smaller lesions were detected by hybrid imaging. (E) Representative maximum-intensity projections of patient with multiple lesions. On left are lesions reported on hybrid imaging (green); on right, lesions reported on CT or MRI alone (red).

in the normal adrenal glands and surrounding liver tissue. Furthermore, hybrid ^{18}F-flubrobenguane PET/CT or PET/MRI led to greater diagnostic certainty than morphologic imaging with CT or MRI alone. Particularly, lesions smaller than 1 cm were more often found to be suggestive of pheochromocytoma or paraganglioma with ^{18}F-flubrobenguane PET than with morphologic imaging alone.

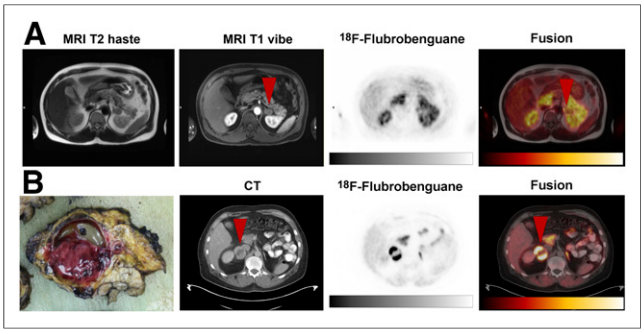

FIGURE 4. Case examples of adrenal adenoma and pheochromocytoma. (A) A 50-y-old man with hypertension and unclear lesion in left adrenal gland. ^{18}F-flubrobenguane PET/CT showed only mild tracer uptake (arrowheads), and surgical resection diagnosed aldosterone-producing adenoma. (B) A 57-y-old man with pathologically elevated metanephrine concentration in plasma. Pheochromocytoma (arrowheads) was detected in right adrenal gland on ^{18}F-flubrobenguane PET/CT by increased tracer uptake in lesion but focal lack of uptake in central necrotic tissue, as was verified after surgical resection. haste = half-Fourier-acquired single-shot turbo spin echo.

Although various PET tracers are already available for the assessment of pheochromocytomas or paragangliomas, such as ^{11}C-hydroxyephedrine, ^{18}F-fluorodopa, ^{18}F-fluorodopamine, or ^{124}I MIBG, these tracers have not found their way into clinical routine because of various disadvantages such as a short half-life or complex radiosynthesis. Accordingly, in the clinical setting, ^{123}I- or ^{131}I-MIBG SPECT/CT, ^{18}F-FDG, or somatostatin receptor–targeted imaging (e.g., ^{68}Ga-DOTATATE) are usually used, all of which demonstrate a rather low sensitivity or specificity. Previously published data favor ^{68}Ga-DOTATATE over ^{18}F-FDG because of a higher lesion-to-background contrast than, and a similar detection rate to, ^{123}I-MIBG SPECT/CT. However, the somatostatin receptor is not a specific target of pheochromocytoma and paraganglioma (*13,20,21*).

Because of its broad availability, iodine-labeled MIBG is the most applied radiotracer for pheochromocytoma and paraganglioma SPECT/CT. MIBG is a guanethidine analog with structural similarities to norepinephrine (*22*) and is often used for imaging of adrenal neoplasms (especially pheochromocytoma, paraganglioma, and neuroblastoma). For imaging purposes, the radionuclide ^{123}I has advantages over ^{131}I, imposing a lower radiation burden on the patient and having superior image quality and higher sensitivity and specificity (*23–25*). On the downside, MIBG SPECT/CT has lower image quality and low tracer-to-background ratios, no quantitative capability, and often a need for multiple acquisition time points (4 and 24 h after injection), resulting in only limited patient comfort and compliance. Consequently, there is a yet-unmet clinical need for feasible PET tracers not just for primary staging and diagnosis but for assessment of therapy response and follow-up examinations.

In the last couple of years, ^{18}F-flubrobenguane has gained more attention, especially for cardiac sympathetic innervation imaging, and its application (mostly in small animals) has been thoroughly described (*15–18,26–29*). These findings underline the potential clinical application of this tracer. Further, the first in vivo studies showed that ^{18}F-flubrobenguane is a suitable PET tracer for pheochromocytoma in a MENX model and therefore interesting for clinical applications (*16*).

PET imaging has multiple major advantages over ^{123}I- or ^{131}I-MIBG SPECT, such as better imaging quality, faster acquisitions at a single time point at a comparable effective dose, and the possibility of true quantification (*17,30*). With these advantages in view, ^{18}F-flubrobenguane combines both PET imaging and a MIBG analog, which might allow an evaluation of therapy response or progressive disease on follow-up examinations superior to that possible with previous methods (*31–33*).

To our knowledge, this work was the first to evaluate ^{18}F-flubrobenguane as a diagnostic tool in patients with suspected pheochromocytoma or paraganglioma. Because of the relatively small cohort of subjects, the scope of this work did not include an

evaluation of the diagnostic accuracy (e.g., sensitivity and specificity) of this new diagnostic modality; rather, the work assessed its principal applicability in this patient population. All patients with histopathologically proven pheochromocytoma or paraganglioma were judged positive on ^{18}F-flubrobenguane PET, indicating high potential for further clinical assessment.

We showed that ^{18}F-flubrobenguane is a suitable PET tracer in pheochromocytomas and paragangliomas, with excellent imaging quality and a high tracer-to-background ratio. Significantly higher tracer uptake was seen in tumor lesions than in healthy adrenal glands and liver parenchyma, making it easier for readers to discriminate pathologic tracer uptake in the adrenal from the liver parenchyma or the contralateral normal adrenal gland. Additionally, our limited reader data hint that ^{18}F-flubrobenguane PET hybrid imaging can be beneficial in detecting smaller tumor lesions with greater certainty than is possible with conventional imaging. Of course, this possibility needs to be validated in larger cohorts or even prospective trials.

Further studies are warranted to investigate the performance of ^{18}F-flubrobenguane in larger clinical trials, particularly with a head-to-head comparison to ^{123}I-MIBG SPECT and conventional imaging such as MRI and CT, which could result in a change in diagnostic management.

There are several limitations to this retrospective analysis. First, we investigated a small and heterogeneous patient cohort that included patients with suspected or recurrent paraganglioma or pheochromocytoma. Further, in only slightly more than half of the cohort was histopathologic validation possible. In cases without histopathologic results, no defined reference standard was available. This is an inherent problem in negative diagnostic test results and could be solved by follow-up examinations. Consequently, we omitted calculation of sensitivity and specificity. Future—preferably prospective—studies need to investigate whether ^{18}F-flubrobenguane PET really has additional value over established examinations such as CT, MRI, or ^{123}I MIBG SPECT, since this question cannot be answered conclusively in the present retrospective study using a clinical patient group in a real-life scenario.

CONCLUSION

The ^{18}F-labeled catecholamine analog ^{18}F-flubrobenguane represents a promising radiotracer for the detection and staging of pheochromocytomas and paragangliomas. ^{18}F-flubrobenguane provides a stable and reproducible biodistribution with high uptake in tumor lesions. The relatively fast acquisition time and excellent image quality on PET are advantageous for pheochromocytoma and paraganglioma staging, and further applications in other tumor entities (e.g., neuroblastoma) should be investigated as well. Nonetheless, because there have been no thorough comparisons of this novel tracer to other established diagnostic methods (e.g., ^{123}I- or ^{131}I-MIBG SPECT/CT or MRI), its clinical benefits need to be evaluated in larger clinical trials.

DISCLOSURE

No potential conflict of interest relevant to this article was reported.

KEY POINTS

QUESTION: Is the novel sympathetic nerve imaging tracer ^{18}F-flubrobenguane suitable for the evaluation of patients with suspected pheochromocytoma or paraganglioma?

PERTINENT FINDINGS: In 23 patients with suspected pheochromocytoma or paraganglioma, 47 lesions were detected. When ^{18}F-flubrobenguane PET/CT was compared with conventional imaging, more and smaller lesions were described, without reaching statistical significance. A significantly higher tracer accumulation was found in pheochromocytoma or paraganglioma than in the healthy adrenal gland.

IMPLICATIONS FOR PATIENT CARE: ^{18}F-flubrobenguane PET is a promising imaging modality in patients with suspected pheochromocytoma and paraganglioma and should be investigated in larger studies.

REFERENCES

1. Lenders JWM, Eisenhofer G, Mannelli M, Pacak K. Phaeochromocytoma. *Lancet.* 2005;366:665–675.
2. Lenders JWM, Duh Q-Y, Eisenhofer G, et al. Pheochromocytoma and paraganglioma: an Endocrine Society clinical practice guideline. *J Clin Endocrinol Metab.* 2014;99:1915–1942.
3. Modigliani E, Vasen HM, Raue K, et al. Pheochromocytoma in multiple endocrine neoplasia type 2: European study. The Euromen Study Group. *J Intern Med.* 1995;238:363–367.
4. Lonser RR, Glenn GM, Walther M, et al. von Hippel-Lindau disease. *Lancet.* 2003;361:2059–2067.
5. Gruber LM, Erickson D, Babovic-Vuksanovic D, Thompson GB, Young WF, Bancos I. Pheochromocytoma and paraganglioma in patients with neurofibromatosis type 1. *Clin Endocrinol (Oxf).* 2017;86:141–149.
6. Waguespack SG, Rich T, Grubbs E, et al. A current review of the etiology, diagnosis, and treatment of pediatric pheochromocytoma and paraganglioma. *J Clin Endocrinol Metab.* 2010;95:2023–2037.
7. Edström Elder E, Hjelm Skog A-L, Höög A, Hamberger B. The management of benign and malignant pheochromocytoma and abdominal paraganglioma. *Eur J Surg Oncol.* 2003;29:278–283.
8. Lloyd R, Osamura R, Kloppel G, Rosai J. *WHO Classification of Tumours: Pathology and Genetics of Tumours of Endocrine Organs.* 4th ed. International Agency for Research on Cancer; 2017:179–206.
9. Welch TJ, Sheedy PF, van Heerden JA, Sheps SG, Hattery RR, Stephens DH. Pheochromocytoma: value of computed tomography. *Radiology.* 1983;148:501–503.
10. Ganguly A, Henry DP, Yune HY, et al. Diagnosis and localization of pheochromocytoma: detection by measurement of urinary norepinephrine excretion during sleep, plasma norepinephrine concentration and computerized axial tomography [CT-scan]. *Am J Med.* 1979;67:21–26.
11. Hicks RJ, Hofman MS. Is there still a role for SPECT-CT in oncology in the PET-CT era? *Nat Rev Clin Oncol.* 2012;9:712–720.
12. Pandit-Taskar N, Modak S. Norepinephrine transporter as a target for imaging and therapy. *J Nucl Med.* 2017;58(suppl):39S–53S.
13. Jing H, Li F, Wang L, et al. Comparison of the ^{68}Ga-DOTATATA PET/CT, FDG PET/CT, and MIBG SPECT/CT in the evaluation of suspected primary pheochromocytomas and paragangliomas. *Clin Nucl Med.* 2017;42:525–529.
14. Green M, Lowe J, Kadirvel M, et al. Radiosynthesis of no-carrier-added meta-[^{124}I]iodobenzylguanidine for PET imaging of metastatic neuroblastoma. *J Radioanal Nucl Chem.* 2017;311:727–732.
15. Yu M, Bozek J, Lamoy M, et al. Evaluation of LMI1195, a novel ^{18}F-labeled cardiac neuronal PET imaging agent, in cells and animal models. *Circ Cardiovasc Imaging.* 2011;4:435–443.
16. Gaertner FC, Wiedemann T, Yousefi BH, et al. Preclinical evaluation of ^{18}F-LMI1195 for in vivo imaging of pheochromocytoma in the MENX tumor model. *J Nucl Med.* 2013;54:2111–2117.
17. Sinusas AJ, Lazewatsky J, Brunetti J, et al. Biodistribution and radiation dosimetry of LMI1195: first-in-human study of a novel ^{18}F-labeled tracer for imaging myocardial innervation. *J Nucl Med.* 2014;55:1445–1451.
18. Zelt JGE, Mielniczuk LM, Orlandi C, et al. PET imaging of sympathetic innervation with [^{18}F]flurobenguan vs [^{11}C]mHED in a patient with ischemic cardiomyopathy. *J Nucl Cardiol.* 2019;26:2151–2153.

19. Giesel FL, Kratochwil C, Lindner T, et al. ^{68}Ga-FAPI PET/CT: biodistribution and preliminary dosimetry estimate of 2 DOTA-containing FAP-targeting agents in patients with various cancers. *J Nucl Med.* 2019;60:386–392.
20. Chang CA, Pattison DA, Tothill RW, et al. ^{68}Ga-DOTATATE and ^{18}F-FDG PET/CT in paraganglioma and pheochromocytoma: utility, patterns and heterogeneity. *Cancer Imaging.* 2016;16:22.
21. Janssen I, Blanchet EM, Adams K, et al. Superiority of [^{68}Ga]-DOTATATE PET/CT to other functional imaging modalities in the localization of SDHB-associated metastatic pheochromocytoma and paraganglioma. *Clin Cancer Res.* 2015;21:3888–3895.
22. Chen CC, Carrasquillo JA. Molecular imaging of adrenal neoplasms. *J Surg Oncol.* 2012;106:532–542.
23. Furuta N, Kiyota H, Yoshigoe F, Hasegawa N, Ohishi Y. Diagnosis of pheochromocytoma using [^{123}I]-compared with [^{131}I]-metaiodobenzylguanidine scintigraphy. *Int J Urol.* 1999;6:119–124.
24. Mattsson S, Johansson L, Leide Svegborn S, et al. ICRP publication 128: radiation dose to patients from radiopharmaceuticals—a compendium of current information related to frequently used substances. *Ann ICRP.* 2015;44:7–321.
25. Van Der Horst-Schrivers ANA, Jager PL, Boezen HM, Schouten JP, Kema IP, Links TP. Iodine-123 metaiodobenzylguanidine scintigraphy in localising phaeochromocytomas: experience and meta-analysis. *Anticancer Res.* 2006;26:1599–1604.
26. Yu M, Bozek J, Lamoy M, et al. LMI1195 PET imaging in evaluation of regional cardiac sympathetic denervation and its potential role in antiarrhythmic drug treatment. *Eur J Nucl Med Mol Imaging.* 2012;39:1910–1919.
27. Higuchi T, Yousefi BH, Kaiser F, et al. Assessment of the ^{18}F-labeled PET tracer LMI1195 for imaging norepinephrine handling in rat hearts. *J Nucl Med.* 2013;54:1142–1146.
28. Yu M, Bozek J, Kagan M, et al. Cardiac retention of PET neuronal imaging agent LMI1195 in different species: impact of norepinephrine uptake-1 and -2 transporters. *Nucl Med Biol.* 2013;40:682–688.
29. Werner RA, Rischpler C, Onthank D, et al. Retention kinetics of the ^{18}F-labeled sympathetic nerve PET tracer LMI1195: comparison with ^{11}C-hydroxyephedrine and ^{123}I-MIBG. *J Nucl Med.* 2015;56:1429–1433.
30. Radiation dose to patients from radiopharmaceuticals (addendum 2 to ICRP publication 53). *Ann ICRP.* 1998;28:1–126.
31. Rahmim A, Zaidi H. PET versus SPECT: strengths, limitations and challenges. *Nucl Med Commun.* 2008;29:193–207.
32. Garcia EV. Physical attributes, limitations, and future potential for PET and SPECT. *J Nucl Cardiol.* 2012;19(suppl 1):S19–S29.
33. Gholamrezanejhad A, Mirpour S, Mariani G. Future of nuclear medicine: SPECT versus PET. *J Nucl Med.* 2009;50(7):16N–18N.